

Dry deposition

One of the processes accounting for removal of heavy metals from the atmosphere is dry deposition. Heavy metals in aerosol composition or in gaseous form interact with ground surface (buildings, trees, grass, soil, water surface etc.). As a result they stick or react with the surface and are removed from the air. Dry deposition of a substance to a particular surface type i is described by the equation:

$$\frac{\partial q}{\partial t} = -\Lambda_{dry}^i q, \quad (1)$$

where Λ_{dry}^i is the surface dependent dry deposition coefficient, proportional to dry deposition velocity V_d^i :

$$\Lambda_{dry}^i = \frac{V_d^i}{\Delta\sigma_1} \left| \frac{\partial\sigma}{\partial z} \right|, \quad \frac{\partial\sigma}{\partial z} = -\frac{g}{R_a T_a} \left(\sigma_1 + \frac{p_t}{p^*} \right). \quad (2)$$

Here $\Delta\sigma_1$ and σ_1 are depth and mid-level of the lowest σ -layer respectively.

The pollutant mixing ratio averaged over a gridcell after the dry deposition is given by:

$$q^{t+\Delta t} = q^t \sum_i f_i \exp(-\Lambda_{dry}^i \Delta t) \quad (3)$$

where f_i is area fraction of a surface type i in a gridcell and summing is performed over all surface types in the cell.

Commonly the dry deposition velocity is calculated using the resistance analogy [e.g. *Wesely and Hicks, 2000*]. For gases it has the following form:

$$V_d^i = \frac{1}{R_a + R_b + R_c}, \quad (4)$$

where R_a is the aerodynamic resistance between a reference height (mid-level of the lowest σ -layer) and the quasi-laminar sub-layer above the surface;

R_b is the quasi-laminar sub-layer resistance;

R_c is the surface resistance to chemical, physical and biological interactions.

Dry deposition velocities of aerosol differ from those of gases (Eq. (4)) by absence of the surface resistance and influence of the gravitational sedimentation [*Seinfeld and Pandis, 1997*]:

$$V_d^i = \frac{1}{R_a + R_b + R_a R_b V_g} + V_g, \quad (5)$$

where V_g is the gravitational sedimentation velocity.

Aerodynamic resistance

The aerodynamic resistance can be approximated from the similarity theory as [Jacobson, 1999]:

$$R_a = \frac{1}{kU_*} \int_{z_{0h}}^{z_{ref}-d} \Phi_h \frac{dz}{z}, \quad (6)$$

where k is the von Kármán constant taken as 0.4;
 u_* is the friction velocity;
 z_{ref} is the reference height (mid-level of the lowest σ -layer);
 d is the displacement height;
 z_{0h} is the energy roughness length; and Φ_h is the dimensionless potential temperature gradient.

The friction velocity is given by:

$$u_* = kU_{ref} \left(\int_{z_{0m}}^{z_{ref}-d} \Phi_m \frac{dz}{z} \right)^{-1}, \quad (7)$$

where U_{ref} is wind velocity at the reference height;
 z_{0m} is the roughness length for momentum;
 Φ_m is the dimensionless wind shear.

The momentum roughness length z_{0m} for different land cover types along with the displacement heights are given in Table 1. The roughness length for water surfaces is a function of the friction velocity [Garratt, 1999]:

$$z_{0m} = \alpha_c u_*^2 / g + 0.11\nu / u_*, \quad (8)$$

where $\alpha_c \approx 0.016$ is the Charnock constant; and ν is the kinematic viscosity of air.

Table 1. Land cover categories of CCE dataset used in the model

1. Temperate coniferous forest	10. Semi-natural
2. Temperate deciduous forest	11. Mediterranean scrub
3. Mediterranean needleleaf forest	12. Wetlands
4. Mediterranean broadleaf forest	13. Tundra
5. Temperate crops	14. Desert/Barren
6. Mediterranean crops	15. Water
7. Root crops	16. Ice
8. Grasslands	17. Urban
9. Wheat	

The energy roughness length is expressed through that of momentum for a wide variety of surfaces [Garratt, 1999]:

$$\ln \left(\frac{z_{0m}}{z_{0h}} \right) \approx \begin{cases} 2 & \text{rough surface} \\ k(13.6Pr^{2/3} - 12) & \text{water surface} \end{cases}, \quad (9)$$

where $Pr = \nu \rho c_{pm} / \kappa$ is the Prandtl number;
 ρ is air density;
 c_{pm} is the specific heat of moist air;
 κ is the thermal air conductivity.

The integrals of Φ_h and Φ_m in Eqs. (6) and (7) are calculated as follows [Jacobson, 1999]:

$$\int_{z_{0h}}^z \Phi_h \frac{dz}{z} = \begin{cases} Pr_t \ln \frac{z}{z_{0h}} + \frac{\beta_h}{L} (z - z_{0h}) & z/L > 0 \quad (stable) \\ Pr_t \left[\ln \frac{(1 - \gamma_h z/L)^{1/2} - 1}{(1 - \gamma_h z/L)^{1/2} + 1} - \ln \frac{(1 - \gamma_h z_{0h}/L)^{1/2} - 1}{(1 - \gamma_h z_{0h}/L)^{1/2} + 1} \right] & z/L < 0 \quad (unstable) \\ Pr_t \ln \frac{z}{z_{0h}} & z/L = 0 \quad (neutral) \end{cases} \quad (10)$$

$$\int_{z_{0m}}^z \Phi_m \frac{dz}{z} = \begin{cases} \ln \frac{z}{z_{0m}} + \frac{\beta_m}{L} (z - z_{0m}) & z/L > 0 \quad (stable) \\ \ln \frac{(1 - \gamma_m z/L)^{1/4} - 1}{(1 - \gamma_m z/L)^{1/4} + 1} - \ln \frac{(1 - \gamma_m z_{0m}/L)^{1/4} - 1}{(1 - \gamma_m z_{0m}/L)^{1/4} + 1} \\ + 2 \tan^{-1} \left(1 - \gamma_m \frac{z}{L} \right)^{1/4} - 2 \tan^{-1} \left(1 - \gamma_m \frac{z_{0m}}{L} \right)^{1/4} & z/L > 0 \quad (unstable) \\ \ln \frac{z}{z_{0m}} & z/L = 0 \quad (neutral) \end{cases} \quad (11)$$

Here $Pr_t \approx 0.95$ is the turbulent Prandtl number;
 $\beta_h = 7.8$; $\gamma_h = 11.6$; $\beta_m = 6.0$; $\gamma_m = 19.3$;
 L is the Monin-Obukhov length.

Gridcell averaged values of the Monin-Obukhov length are supported by the meteorological pre-processor. To obtain values specific for each land cover type we use the following expression for L [Jacobson, 1999]:

$$L = - \frac{c_{pd} \rho \theta_v}{kg H_f} u_*^3, \quad (12)$$

where c_{pd} is the specific heat of dry air;
 θ_v is the potential virtual temperature;
 H_f is the vertical turbulent sensible-heat flux.

The Eqs. (7) and (12) are iterated for u_* and L using the cell averaged values for the initial estimate.

Aerosol deposition

Dry deposition velocities of aerosol is described by Eq. (5), where the gravitational sedimentation velocity V_g is given as follows:

$$V_g = \frac{d_p^2 \rho_p g}{18\eta} G_{cunn} . \quad (13)$$

Here d_p and ρ_p are the aerosol diameter and density respectively;

$G_{cunn} = 1 + Kn (1.249 + 0.42 \exp(-0.87 / Kn))$ is the Cunningham correction factor [Jacobson, 1999];

$Kn = 2\lambda / d_p$ is the Knudsen number; and λ is the mean free path of air molecules.

In the moist atmospheric air condensation of water vapor on aerosol particles leads to increase of their size. The diameter of an aerosol that is in equilibrium with the air moisture depends upon ambient humidity [Fitzgerald, 1975]:

$$d_p = Ad_d^B ; \quad A = 1.2 \exp\left(\frac{0.066S}{1.058 - S}\right); \quad B = \exp\left(\frac{0.00077S}{1.009 - S}\right), \quad (14)$$

where d_d is the dry diameter of an aerosol;

S is the air saturation ratio.

In this parameterization we expect that the water absorbing mass fraction of the aerosol is equal to unity.

Vegetated surfaces

The size-segregated approach developed for dry deposition to vegetated surfaces is based on theoretical work [Slinn, 1982] and fitted to experimental data. Empirical parameterizations based on extensive field measurements [Ruijgrok *et al.*, 1997; Wesely *et al.*, 1985] are used for selection of the model parameters. A similar approach is suggested by L.Zhang *et al.* [2001]. Following [Slinn, 1982] the deposition velocity is expressed in simplified form:

$$V_d^{veg} = \frac{1}{R_a + R_s} + V_g . \quad (15)$$

Here R_s is the resistance of the interfacial sub-layer (the layer within and just above the roughness elements) also called as the 'canopy resistance'.

This resistance is calculated as follows:

$$R_s = \frac{U_h}{EU_*^2}, \quad (16)$$

where E is the total efficiency of particles collection by the surface;

U_h is the wind velocity at the canopy height H given as:

$$U_h = \frac{u_*}{k} \int_{z_{0m}}^{H-d} \Phi_m \frac{dz}{z}. \quad (17)$$

Following *W.G.N.Slinn* [1982] and *L.Zhang et al.* [2001] the collection efficiency has the following form:

$$E = \varepsilon_0(E_b + E_{in} + E_{im})r_{off}, \quad (18)$$

where E_b , E_{in} , E_{im} are constituents of the collection efficiency from Brownian diffusion, interception and impaction respectively;

r_{off} represents reduction of the efficiency caused by particles bounce-off;

ε_0 is the empirical constant taken from fitting to the experimental data.

The diffusion term is given as [*Slinn*, 1982]:

$$E_b = Sc^{-2/3}, \quad (19)$$

where $Sc = \nu / D_p$ is the Schmidt number;

D_p is the particle Brownian diffusion coefficient.

We use a generalized form of the impaction term suggested in [*Peters and Eiden*, 1992]:

$$E_{im} = \left(\frac{St}{\alpha + St} \right)^\beta, \quad (20)$$

where $St = u_* V_g / (g\hat{A})$ is the Stokes number for vegetated surfaces;

\hat{A} is the characteristic collector width given below;

α and β are constants chosen to fit the experimental data.

The interception term is the most uncertain part of the collection efficiency. *W.G.N.Slinn* [1982] parameterized it composing contributions of small (vegetative hairs) and large (grass blades, needles etc.) collectors:

$$E_{in} = F \frac{d_p}{d_p + \check{A}} + (1-F) \frac{d_p}{d_p + \hat{A}}, \quad (21)$$

where \check{A} and \hat{A} are characteristics width of small and large collectors taken as 10 μm and 1 mm respectively;

F and $(1-F)$ are the contributions of these two collector types, where $F = 0.01$.

The choice of these parameters is arbitrary to some extent since there is no experimental or theoretical data on their values. However, the sensitivity analysis has shown that the interception term is insignificant in comparison with two other terms.

The bounce-off correction factor is taken in the form [*Slinn*, 1982]:

$$r_{off} = \exp(-\gamma St^\delta), \quad (22)$$

where γ and δ are the fitting constants.

It is assumed that the particles bounce-off takes place from dry surfaces only. The surface is supposed to be dry if no precipitation occurred during current 6-hours meteorological period for grass and during current and previous periods for forest.

Forests

To evaluate the constants of the deposition scheme described above for tall vegetation (forests) the scheme was fitted to empirical parameterization developed by *W.Ruijgrok et al.* [1997]. This parameterization is based on extensive measurements of dry deposition velocities of aerosol particles over needleleaf and some mixed forests. It takes into account dependence of the dry deposition velocity on the friction velocity and relative humidity of the ambient air. Particles of two size ranges are described: fine fraction with mass median diameter (MMD) = 0.6 μm (NH_4 , SO_4 , NO_3) and coarse fraction with MMD = 5.12 μm (Na). Parameters of dry deposition of different particles in the fine fraction vary insignificantly therefore mean values of the coefficients were used. The fitting constants of the dry deposition scheme obtained for forests are presented in Table 2.

Table 2. Empirical constants of the dry deposition scheme for vegetated surfaces

Constant	Forests	Low vegetation
α	1	1
β	0.5	0.5
γ	2	2
δ	0.25	0.25
ε_0	1.4	0.22
A	–	100

A comparison of the collection efficiency of the Ruijgrok's parameterization with the model scheme is shown in Figs. 1 and 2 for particles with $d_p = 0.6 \mu\text{m}$ over a wet surface. As seen both schemes give similar functional dependencies on the ambient air relative humidity and the friction velocity. The model scheme predicts more intensive increase of the collection efficiency for relative humidity close to 100%. Similar results are also obtained for a dry surface and for particles with $d_p = 5.12 \mu\text{m}$.

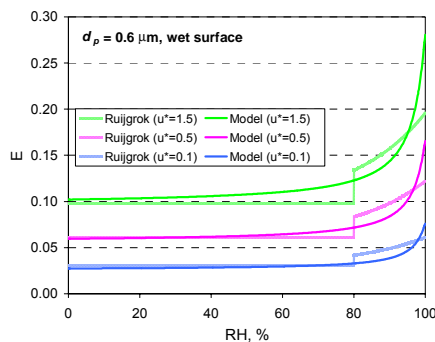


Fig.1 Collection efficiency over forest (wet surface) as a function of the ambient air relative humidity

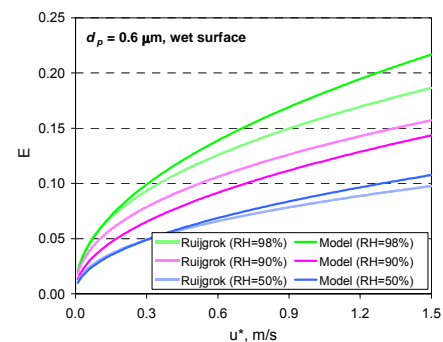


Fig. 2. Collection efficiency over forest (wet surface) as a function of the friction velocity

Figs. 3 and 4 shows the dry deposition velocity of aerosol particles over wet and dry forest surface respectively as a function of a particle size. The solid line presents the model scheme, filled squares show the Ruijgrok's parameterization for particles with MMD 0.6 μm and 5.12 μm . As seen from the figures both schemes are in good agreement. The dry deposition velocity of coarse particles over a dry surface is somewhat lower than that over a wet surface because of the bounce-off effect. Besides, the model scheme was tested using the full set of meteorological data. Fig. 5 shows the cumulative distribution function of dry deposition velocity over coniferous forests in Europe obtained for the year

2000 by the model scheme and the Ruijgrok's parameterization. As seen from the figure the results practically coincide.

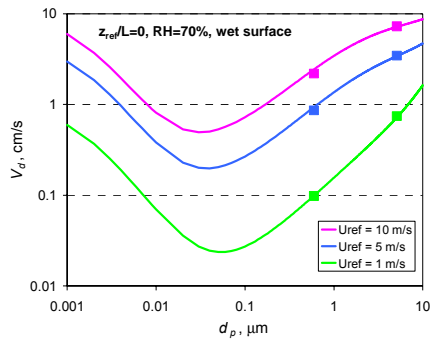


Fig. 3. Dry deposition velocity to forest (wet surface) as a function of a particle size. Solid lines show the model results, the filled squares depict the Ruijgrok's parameterization

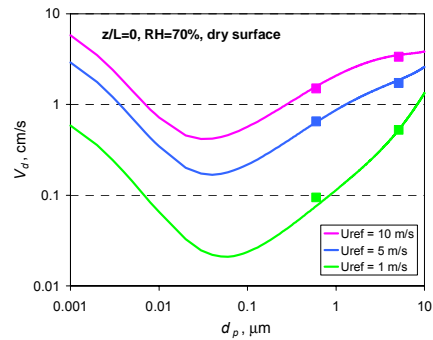


Fig. 4. Dry deposition velocity to forest (dry surface) as a function of particle size. Solid lines show the model results, the filled squares depict the Ruijgrok's parameterization

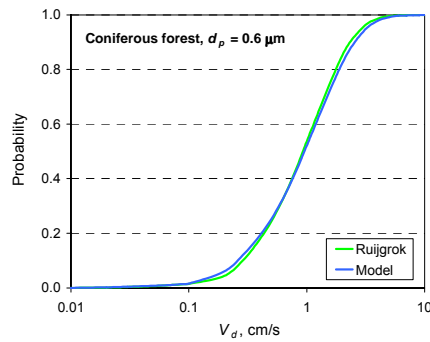


Fig. 5. Cumulative distribution function of dry deposition velocity over coniferous forests in Europe

Low vegetation

For low vegetation (grassland, crops, wetland etc.) a procedure similar to that described above was used to evaluate the constants of the dry deposition scheme. The scheme was fitted to the empirical parameterization developed from field measurements of particles dry deposition to grass [Wesely *et al.*, 1985]. The expression for the interfacial sub-layer resistance Eq.(16) was modified to take into account the atmospheric stability conditions as suggested by M.L.Wesely *et al.* [1985]:

$$R_s = \begin{cases} \frac{U_h}{Eu_*^2} & L \geq 0 \\ \frac{U_h}{Eu_*^2} \left[1 + \left(-\frac{A}{L} \right)^{2/3} \right]^{-1} & L < 0 \end{cases}, \quad (23)$$

where A is a fitting constant.

Values of the fitting constants of the model dry deposition scheme for low vegetation are presented in Table 2. Fig. 6 shows the comparison of the model scheme for grass with the Wesely's parameterization. As seen the interfacial sub-layer conductivity (reciprocal resistance) given by the Wesely's parameterization lies between those predicted by the model for dry and wet surfaces. The dry deposition velocity over grass (dry surface) as a function of a particle size is illustrated in Fig. 7. The cumulative distribution function of dry deposition velocity over grassland in Europe for conditions

of 2000 is shown in Fig. 8. As seen from the figure the model somewhat underestimates the Wesely's parameterization for small deposition velocities.

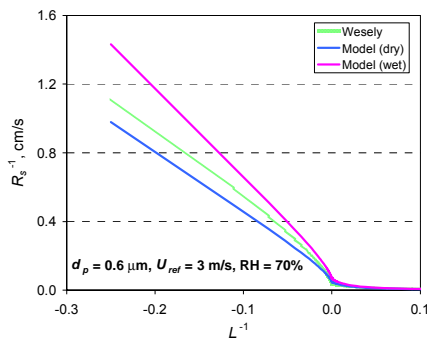


Fig. 6. Reciprocal resistance of the interfacial sub-layer over grass as a function of the stability conditions

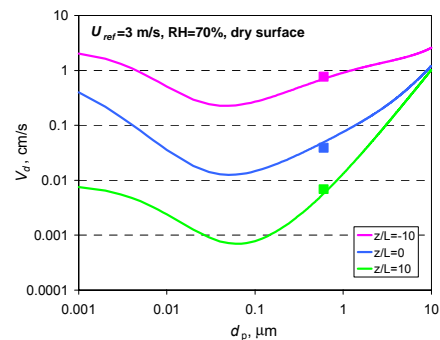


Fig. 7. Dry deposition velocity to grass (dry surface) as a function of particle size. Solid lines show the model results, the filled squares depict the Ruijgrok's parameterization

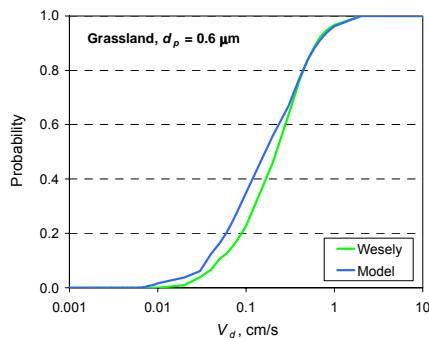


Fig. 8. Cumulative distribution function of dry deposition velocity over grassland in Europe

Water surface

The parameterization of dry deposition to water surfaces is based on the approach suggested by *R.M. Williams* [1982] taking into account the effects of wave breaking and aerosol washout by seawater spray. A similar approach was developed in [*Pryor et al.*, 1999]. The modified resistance scheme of aerosol particles dry deposition over water surface is illustrated in Fig. 9. Following the procedure from [*Williams*, 1982] one can obtain an expression for the dry deposition velocity:

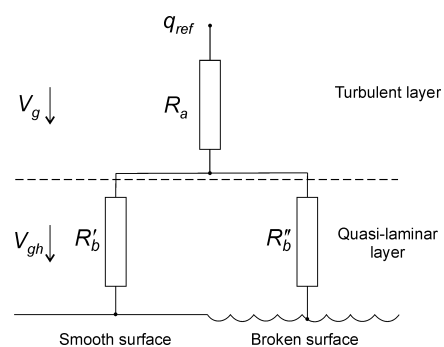


Fig. 9. Resistance scheme of aerosol particles dry deposition over water surface

$$V_d^{water} = \frac{(1 + R_a V_g)(1 + R_b V_{gh})}{R_a + R_b + R_a R_b V_{gh}}, \quad (24)$$

where V_{gh} is the gravitational sedimentation velocity in the humid quasi-laminar layer near the air-water interface.

The relative air humidity of this layer can be significantly higher than that of the turbulent layer. It results in more intensive particle growth. Since due to Raoult's law the relative humidity over salt water cannot exceed 98.3%, the constant value of 98% is accepted in the model for the humid layer. The quasi-laminar layer resistance R_b consists of the resistance over the smooth surface R'_b and the resistance over the broken one R''_b :

$$R_b = \left(\frac{1 - \alpha_b}{R'_b} + \frac{\alpha_b}{R''_b} \right). \quad (25)$$

Here α_b is the fraction surface area broken due to the wind force [Wu, 1979]:

$$\alpha_b = 1.7 \cdot 10^{-6} U_{10}^{3.75}, \quad (26)$$

where U_{10} is the wind speed at 10 m height.

The quasi-laminar layer resistance over the smooth surface is determined mostly by the Brownian diffusion and impaction [Slinn and Slinn, 1980]:

$$R'_b = \frac{k U_{ref}}{u_*^2} (E_b + E_{im})^{-1}, \quad E_b = Sc^{-1/2}, \quad E_{im} = 10^{-3/St}, \quad (27)$$

where the Stokes number for water surfaces is $St = u_*^2 V_{gh} / (g \nu)$;

the Schmidt number is $Sc = \nu / D_{ph}$, D_{ph} is the diffusion coefficient in the humid layer.

The broken surface resistance R''_b governed by scavenging of particles due to impaction and coagulation with spray droplets is expected to be quite low. Because of lack of reliable estimates for this resistance a tentative value of 10 s/m [Williams, 1982] is used. Fig. 10 illustrates the velocity of dry deposition to water surface as a function of particle size for different values of wind speed. The influence of the broken surface resistance on the dry deposition velocity over water surfaces is illustrated in Fig. 11. The lowest case corresponds to water surface with no broken area.

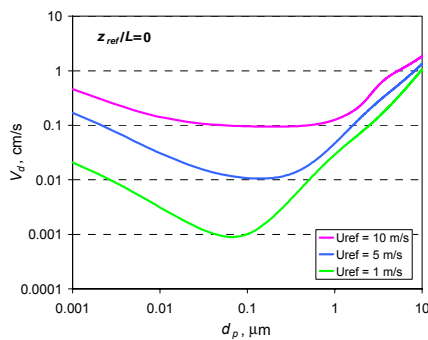


Fig. 10. Dry deposition velocity to water surface as a function of particle size for different values of wind speeds

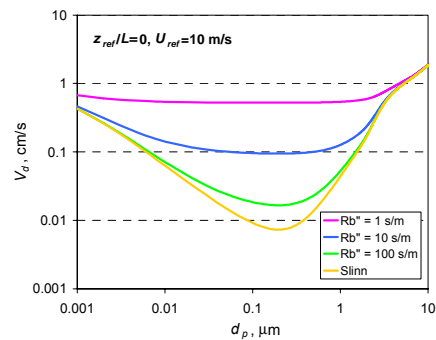


Fig. 11. Dry deposition velocity to water surface as a function of particle size for different values of the broken surface resistance

Non-vegetated surfaces

The dry deposition to non-vegetated surfaces (deserts, glaciers etc.) is described by Eq.(5), where the resistance of the quasi-laminar layer has the following form:

$$R_b = \frac{kU_{ref}}{u_*^2} (E_b + E_{im})^{-1} \quad , \quad E_b = Sc^{-2/3} \quad , \quad E_{im} = 10^{-3/St} \quad . \quad (28)$$

The Schmidt and the Stokes numbers are $Sc = \nu/D_p$ and $St = u_*^2 V_g / (g\nu)$ respectively. The particular case of non-vegetated surfaces is urban area characterized by bluff roughness elements. For urban areas we used a different form of the impaction term $E_{im} = St^2 / (400 + St^2)$ [Giorgi, 1986].

Fig. 12 shows dry deposition velocities of particles with $d_p = 0.6 \mu\text{m}$ to different land cover categories in the EMEP region calculated for meteorological conditions of 2000. As seen the highest deposition velocities correspond to forests (around 1 cm/s), whereas the lowest – to barren land and permanent ice areas (glaciers) (below 0.01 cm/s on average).

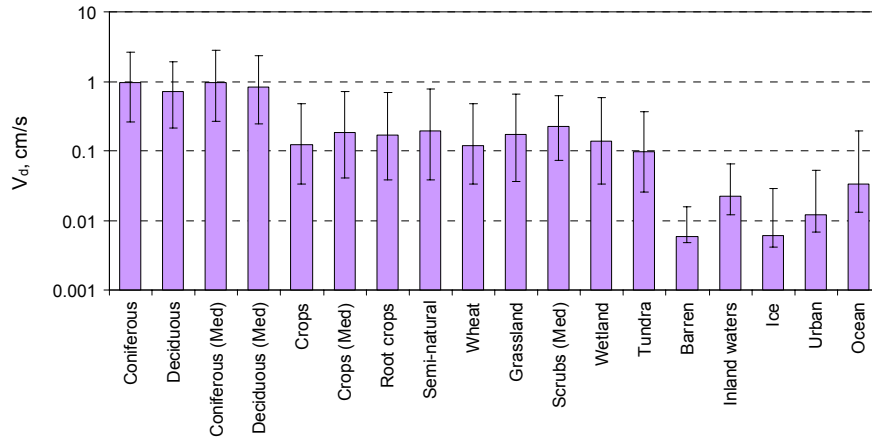


Fig. 12. Dry deposition velocities of particles ($d_p = 0.6 \mu\text{m}$) to different land cover categories in the EMEP region. Bars show median values of 6-hour averages during 2000. Error bars depict 90%-confidence intervals

The current version of the model describes particles carrying heavy metal as mono-disperse fraction with appropriate MMD: Pb – $0.55 \mu\text{m}$, Cd – $0.84 \mu\text{m}$, Hg – $0.61 \mu\text{m}$ [Milford and Davidson, 1985].

Reactive gaseous mercury deposition

The dry deposition of reactive gaseous mercury (RGM) is described by Eq. (4). The quasi-laminar resistance is given as follows [Erisman et al., 1994]:

$$R_b = \frac{2}{ku_*} \left(\frac{Sc}{Pr} \right)^{2/3} \quad , \quad (29)$$

where Schmidt number $Sc = \nu / D_g$;

D_g is the molecular diffusion coefficient of RGM.

Since solubility of RGM is similar to those of nitric acid vapor [Petersen et al., 1995] the surface resistance R_c is taken to be zero [Wesely and Hicks, 2000].

Dry deposition velocities of RGM to different land cover categories in the EMEP region calculated for meteorological conditions of 2000 are shown in Fig. 13. The highest deposition velocities are to forests and urban areas (3 cm/s on average), the lowest velocities are to inland waters (0.5 cm/s).

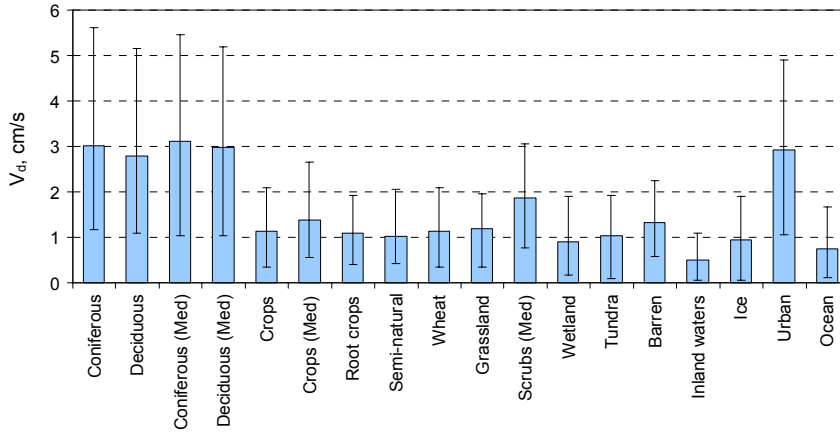


Fig. 1.17. Dry deposition velocities RGM to different land cover categories in the EMEP region. Bars show median values of 6-hour averages during 2000. Error bars depict 90%-confidence intervals

Gaseous elemental mercury deposition

Dry deposition of elemental gaseous mercury by various types of underlying surface is not adequately defined yet. Some experts [US EPA, 1997] suppose that this type of mercury removal is not an essential sink on a regional and global scale. According to another viewpoint [Lin and Pehkonen, 1999] dry uptake of elemental mercury is considered to be the dominating mechanism of mercury removal from the atmosphere. Summarizing available literature data [Travnikov and Ryaboshapko, 2002] we adopt the following simplified parameterization of the process. There is no dry uptake of elemental gaseous mercury by water surface and land surface not covered by vegetation. It is also absent during nighttime. Over the vegetated surface during daytime dry deposition velocity is given by:

$$V_d^{veg} = \begin{cases} 0, & T_s \leq T_0 \\ B \frac{T_s - T_0}{T_1 - T_0} \cos \theta_s, & T_0 < T_s \leq T_1 \\ B \cos \theta_s, & T_s > T_1 \end{cases}, \quad (30)$$

where T_s is the surface temperature, $T_0 = 273K$ and $T_1 = 293K$;

B is equal to 0.03 cm/s for forests and 0.01 cm/s for low vegetation;

θ_s is the solar zenith angle calculated according to [Jacobson, 1999].

Fog deposition

Mercury aqueous forms in fog droplets can be removed from the atmosphere through the fog interaction with the ground surface. The fog dry deposition is described in the model similar to that of aerosol particles with mass median diameter 20 μm .